European Journal of Pharmaceutics and Biopharmaceutics 198 (2024) 114270

Contents lists available at ScienceDirect

European Journal of Pharmaceutics and Biopharmaceutics

journal homepage: www.elsevier.com/locate/ejpb

Research paper

# Development of a simple paste for 3D printing of drug formulations containing a mesoporous material loaded with a poorly water-soluble drug

Christos S. Katsiotis [a], Evgenii Tikhomirov [a], Christos Leliopoulos [b], Maria Strømme [a], Ken Welch [a,*]

[a] Division of Nanotechnology and Functional Materials, Department of Materials Science and Engineering, Uppsala University, Box 35, Uppsala SE-751 03, Sweden
[b] Division of Macromolecular Chemistry, Department of Chemistry, Uppsala University, Box 538, SE-751 21, Sweden

ARTICLE INFO

*Keywords:*
3D printing
Additive manufacturing
Semi Solid Extrusion
Paste
Mesoporous Magnesium Carbonate
Poorly soluble drug
Drug delivery

ABSTRACT

Poorly soluble drugs represent a substantial portion of emerging drug candidates, posing significant challenges for pharmaceutical formulators. One promising method to enhance the drug's dissolution rate and, consequently, bioavailability involves transforming them into an amorphous state within mesoporous materials. These materials can then be seamlessly integrated into personalized drug formulations using Additive Manufacturing (AM) techniques, most commonly via Fused Deposition Modeling. Another innovative approach within the realm of AM for mesoporous material-based formulations is semi-solid extrusion (SSE). This study showcases the feasibility of a straightforward yet groundbreaking hybrid 3D printing system employing SSE to incorporate drug-loaded mesoporous magnesium carbonate (MMC) into two different drug formulations, each designed for distinct administration routes. MMC was loaded with the poorly water-soluble drug ibuprofen via a solvent evaporation method and mixed with PEG 400 as a binder and lubricant, facilitating subsequent SSE. The formulation is non-aqueous, unlike most pastes which are used for SSE, and thus is beneficial for the incorporation of poorly water-soluble drugs. The 3D printing process yielded tablets for oral administration and suppositories for rectal administration, which were then analyzed for their dissolution behavior in biorelevant media. These investigations revealed enhancements in the dissolution kinetics of the amorphous drug-loaded MMC formulations. Furthermore, an impressive drug loading of 15.3 % w/w of the total formulation was achieved, marking the highest reported loading for SSE formulations incorporating mesoporous materials to stabilize drugs in their amorphous state by a wide margin. This simple formulation containing PEG 400 also showed advantages over other aqueous formulations for SSE in that the formulations did not exhibit weight loss or changes in size or form during the curing process post-printing. These results underscore the substantial potential of this innovative hybrid 3D printing system for the development of drug dosage forms, particularly for improving the release profile of poorly water-soluble drugs.

## 1. Introduction

A challenging task for both the pharmaceutical industry and research community is creating formulations of poorly soluble drugs. A large portion of the marketed and newly developed drugs fall within the Biopharmaceutics Classification System (BCS) types II or IV, i.e., substances with either low solubility and high permeability or both low solubility and permeability [1,2]. Various strategies have been employed to overcome solubility and dissolution rate issues of crystalline drugs and consequently increase their bioavailability. For example, amorphous solid dispersions, complexation, particle size reduction, nanosuspensions and pro-drugs have all frequently been used [3,4].

Alternatively, a crystalline drug can be amorphized via incorporation within the pores of a mesoporous material [5–7], which results in a faster dissolution as there are no strong crystalline bonds to overcome. Equally important is the chemical stability for the drug offered by such systems [8]. The amorphization of the drug is achieved due to the high surface area of the mesoporous material and its inner pore volume where the drug is adsorbed and physically constrained, thus inhibiting its recrystallization [9]. Following the release of the formulation in media,

* Corresponding author.
*E-mail addresses:* christos.katsiotis@angstrom.uu.se (C.S. Katsiotis), evgenii.tikhomirov@angstrom.uu.se (E. Tikhomirov), christos.leliopoulos@kemi.uu.se (C. Leliopoulos), maria.stromme@angstrom.uu.se (M. Strømme), ken.welch@angstrom.uu.se (K. Welch).

https://doi.org/10.1016/j.ejpb.2024.114270
Received 10 January 2024; Received in revised form 11 March 2024; Accepted 23 March 2024
Available online 26 March 2024

the drug can achieve supersaturation concentration levels due to its amorphous nature, and hence precipitation inhibitors or stabilizers may be needed to avoid quick recrystallization of the drug [10].

The most commonly used mesoporous materials are silica-based, such as MCM-41, MCM-48 and SBA-15, where MCM-41 is the one most frequently seen in the literature [11,12]. They are typically synthesized utilizing a template strategy in which surfactants are used as structure-directing agents forming micelles that are covered by the silica source. The surfactant is subsequently removed via calcination, leaving behind the porous silica structure [13]. The properties of these materials, such as the pore width, surface area and pore volume, are heavily dictated by the synthesis parameters. For MCM-41 specifically, the pores are typically hexagonal with a width in the range from 1.5 to 10 nm, while the specific surface area is usually between 600 and 1200 $cm^2/g$ [14,15].

An alternative choice for a mesoporous material for drug delivery is mesoporous magnesium carbonate (MMC), which is synthesized with a template-free method employing MgO, methanol and $CO_2$ under pressure [16,17]. MMC's specific surface area (~300–800 $cm^2/g$) and pore size distribution (2–20 nm) can be tuned via the synthesis process [6,18,19]. The long-term chemical stability of a drug loaded in the pores of MMC has also been investigated [19].

Although the peroral route is the predominant of administering drug formulations, other routes of administrations such as nasal, oral (in the mouth) and rectal are employed as well. The formulation for each route requires a specific fabrication technique for the desired administration, i.e. tablets, capsules, aerosols, suppositories, etc. Additive manufacturing (AM), an umbrella of novel manufacturing techniques, can address the limitations of traditional drug formulation manufacturing methods and further improve the development of patient-tailored dosage forms with unique characteristics [20]. A wide range of AM techniques have been investigated for drug delivery applications; however, fused deposition modeling (FDM) is the most prominent one [21].

A combinatorial approach incorporating FDM and drug-loaded mesoporous materials was previously shown to address the low bioavailability of poorly soluble drugs, achieving tunable release kinetics and supersaturation of the drug [22]. However, the addition of non-melting materials, such as the mesoporous materials, in the mixture can negatively affect the mechanical properties of the filaments, as well as limit the number of thermoplastic polymers suitable for this application [23]. To overcome this issue, different AM techniques can be utilized. For example, drug-loaded mesoporous silica has been successfully printed via inkjet printing [24]. Furthermore, semi-solid extrusion (SSE) was also successfully employed for the development of 3D-printed films containing drug-loaded mesoporous silica [25,26]. SSE offers a wide range of solvents and/or hydrogels as excipients. The printing usually takes places at room temperature, therefore eliminating the risk of degradation for thermolabile substances, which is an issue that often plagues the FDM technique. On the other hand, the rheological properties of the stock material can present printing difficulties with SSE, but this can be addressed by the appropriate choice of excipients and dispersion conditions [27].

In this study, we introduce an innovative and straightforward platform for crafting diverse formulations of poorly soluble drugs through SSE. We employed the poorly soluble model drug ibuprofen, classified under BCS category II, by encapsulating it within the pores of MMC. These loaded particles were then blended with a single excipient, PEG 400, to create a paste, subsequently utilized for 3D printing via SSE. This methodology led to the creation of two distinct dosage forms: tablets and suppositories, demonstrating the platform's adaptability for developing drug formulations for different routes of administration.

## 2. Materials and methods

### 2.1. Materials

Mesoporous Magnesium Carbonate (MMC) with a particle size <100 μm was kindly provided by Disruptive Materials AB (Uppsala, Sweden). Monobasic sodium phosphate ($NaH_2PO_4$), dibasic sodium phosphate ($Na_2HPO_4$), PEG 400, Hydrochloric acid (HCl) and sodium chloride (NaCl) were purchased from Merck Life Science AB (Solna, Sweden). Ibuprofen was purchased from Toronto Research Chemicals (Toronto, Canada). Ethanol absolute >99.8 % was purchased from VWR International (Stockholm, Sweden).

### 2.2. Preparation of mesoporous magnesium carbonate (MMC)

Prior to characterization and further use, the raw MMC was heat-treated in a furnace with a 10-hour ramp to 250 °C and an additional 10-hour hold at that temperature, in order to remove any organic intermediate residuals from the synthesis process.

### 2.3. Drug loading of MMC

The drug loading of ibuprofen in MMC was performed via the solvent evaporation technique. A target loading of ibuprofen was selected to be 90 % of the available empty pore volume of MMC. To achieve this loading, 6.5 g of ibuprofen was dissolved in 500 mL of ethanol, and then 15 g of MMC was added and the mixture was directly placed in a rotary evaporator until the solvent was removed. The solid residue was collected and dried in an oven at 70 °C overnight.

### 2.4. Scanning electron microscopy (SEM)

The morphology of MMC before and after being loaded with ibuprofen was examined with electron microscopy. The samples were first sputter-coated with Au/Pd to reduce charging effects. They were subsequently imaged with a LEO 1550 SEM (Zeiss, Jena, Germany) at an acceleration voltage of 5.0 kV.

### 2.5. Gas sorption analysis

Nitrogen gas sorption measurements were performed using an ASAP 2020 (Micromeritics Norcross, GA, USA). Isotherms for samples of both unloaded and drug-loaded MMC were recorded at liquid nitrogen temperature (−196 °C) over a relative pressure range ($p/p_0$) 0 to 1. The samples were first degassed using a Micromeritic SmartVac Prep unit under dynamic vacuum (1 × 10–4 Pa) for 16 h at 70 °C. Values describing the specific surface area (SSA), pore size distribution and total pore volume were calculated using MicroActive Version 5 software (Micromeritics, Norcross, GA, USA). The SSA was calculated using the Brunauer-Emmett-Teller (BET) model, over the relative pressure range of 0.05 to 0.25. The pore size distribution was generated using density functional theory (DFT) to analyze the nitrogen sorption isotherms. Finally, the total pore volume was measured through a single point adsorption at a relative pressure $p/p_0 = 0.985$.

### 2.6. Paste preparation and printability assessment

Pastes of drug-loaded MMC particles with PEG 400 in different ratios were prepared by manual mixing in a mortar. Specifically, the following mass ratios of loaded MMC/PEG 400 were tested: 50/50, 55/45, 60/40 and 65/35. Furthermore, the mixtures of unloaded MMC/PEG 400 at 40/60 and 50/50 were also tested. Subsequently, the pastes were loaded in plastic single-use syringes and their printability was assessed via manually pushing the plunger to extrude material. The characteristics that were evaluated empirically were the extrudability, the flowability and the ability of the extruded paste to be layered without collapsing.

### 2.7. Rheological properties

Viscosity measurements were conducted using a Discovery Hybrid Rheometer-2 (TA instruments, Sollentuna, Sweden). The rheometer was equipped with parallel 20 mm diameter stainless steel geometry, and the measuring gap was set to 1000 μm. Prior to each measurement, a sample trim was performed at a trim gap of 1050 μm to ensure accurate and consistent results. Measurements were carried out at a temperature of 25 °C, and a logarithmic sweep was employed, spanning a range of shear rates from 0.01 to 20 (1/s). This sweep allowed for the characterization of the viscosity of the sample across a broad spectrum of shear rates, enabling a comprehensive understanding of the material's flow behavior. Additionally, the long-term stability and temporal evolution of the viscosity of a selected sample were determined by measurements made at time intervals of 0, 1, 2 and 5 days. To ensure the accuracy and reliability of the viscosity measurements, appropriate calibration procedures were followed, and measurements were performed in triplicate and the average values along with standard deviations were calculated.

### 2.8. 3D-printing of tablets and suppositories

Design of the 3D models of the tablet and suppository were made in Fusion 360 (Autodesk, San Francisco, USA) and then transferred to Simplify 3D (Simplify3D, Cincinnati, USA) for the printing protocol generation. The tablet size was set at 4 mm height and 12 mm diameter, while for the suppository a "bullet" shape was chosen as a cylinder with a rounded top having a diameter of 10 mm and height of 25 mm. The final G-code file was created with the following parameters: Layer height = 0.15 mm; infill type = radial; infill percentage = 100 %; printing speed = 12.5 mm/s; printing surface temperature = room temperature; printhead temperature = room temperature.

Following the printability and rheological assessments described in Sections 2.5 and 2.6, the best performing paste composition was selected for printing of the formulations. A modified ToolChanger and Motion system (E3D-online Ltd, Chalgrove, United Kingdom) was used for 3D-printing of the formulations where an additional syringe pump was integrated as an active tool head for Semi-Solid Extrusion (SSE). Five milliliters Luer Lock tip syringes (Terumo Corporation, Tokyo, Japan) were used as prefilled cartridges mounted into the active tool head. Metcal 916125-DHUV 16-gauge tapered tips with an inner diameter of 1.2 mm (Elfa Distrelec AB, Kista, Sweden) were used as extrusion nozzles. Following the printing of the objects, the samples were stored overnight at room temperature for hardening/curing.

### 2.9. Differential scanning calorimetry (DSC)

DSC measurements were performed on approximately 10 mg samples in perforated aluminum crucibles on a DSC 3 + instrument (Mettler Toledo, Schwerzenbach, Switzerland). The samples were first cooled to −35 °C and heated afterwards to 300 °C at a rate of 10 °C/min.

### 2.10. Thermogravimetric analysis (TGA)

TGA was performed using a TGA/DSC 3+ (Mettler Toledo, Schwerzenbach, Switzerland). Samples weighing 15–20 mg were loaded on uncovered alumina crucibles. They were heated from room temperature to 700 °C at a rate of 10 °C/min in air atmosphere.

### 2.11. Drug loading determination

The drug loading percentage of the developed formulations was also determined experimentally. Approximately 40 mg of drug-loaded MMC powder were dissolved in ethanol. The printed tablet and suppository were also dissolved in ethanol. The concentration of ibuprofen in these formulations was measured at 263 nm with a UV–Vis spectrophotometer (1800, Shimadzu Corporation, Kyoto, Japan). All experiments were performed in triplicate.

### 2.12. In vitro release studies

The *in vitro* release for both printed samples was performed in a USP II apparatus, on a Sotax AT7 (Sotax AG, Aesch, Switzerland). For the tablet samples, which are intended for oral administration, simulated gastric fluid (SGF; NaCl 2 g/L, 1 M HCl 80 mL/L), pH 1.2 was used as dissolution medium [28]. To better simulate rectal administration of the suppository samples, phosphate buffer 100 mM (PB; $Na_2HPO_4$ 13.78 g/L, $NaH_2PO_4$ 3.52 g/L), pH 7.4 was used [29]. Each vessel contained 900 mL of the respective biorelevant medium and was maintained at 37 °C and stirred at 100 rpm. At predetermined time intervals, 3 mL aliquots were removed and the same volume of fresh buffer, kept at 37 °C, was added. The aliquots were filtered through 0.45 μm PTFE filters and ibuprofen absorbance was measured at 263 nm with a UV–vis spectrophotometer (1800, Shimadzu Corporation, Kyoto, Japan). Samples of crystalline ibuprofen with the equivalent dosage contained in the tablet and the suppository samples were also studied in the respective media and compared to the aforementioned samples. As blank experiments, samples containing an equivalent amount of PEG 400 and unloaded MMC were measured to check for background absorbance. All experiments were performed in triplicate.

## 3. Results and discussion

### 3.1. Gas sorption measurements

The nitrogen adsorption and desorption isotherms along with the pore size distribution for the unloaded and the drug-loaded MMC are presented in Fig. 1. The isotherms exhibit a typical type IV shape, in agreement with previous results [5,30]. Table 1 displays the specific surface area (SSA), pore volume and pore width of the MMC before and after loading it with ibuprofen. As expected, all of these parameters decrease post-loading as ibuprofen is filling the internal volume of the mesoporous material.

A high degree of drug loading was desired in this study, and our previous results have shown that the solvent evaporation method is accurate and efficient enough to achieve a targeted drug loading [23]. The amount of ibuprofen used to achieve the desired loading of 90 % of the available pore volume was calculated based on the measured pore volume of the unloaded MMC (0.43 $cm^3/g$) and the molar volume of 200.3 $cm^3$ for ibuprofen [31]. Subsequently, the measured pore volume of the loaded MMC showed a pore volume of 0.05 $cm^3/g$, which provides an indirect measurement of the loading degree of 88.4 %, in excellent agreement with the targeted loading, and corresponds to a 28.1 w/w % of ibuprofen to MMC. These data suggest that most, if not all, of the drug that was used in the loading procedure was loaded within the pores of MMC.

### 3.2. Morphological assessment

SEM imaging of MMC showed a large variability in particle size, which can be expected as the material is formed by the aggregation of smaller nanoparticles [18], and post-synthesis the material was ground and sieved through a 100 μm sieve. The size of the particles varies between below 1 μm up to several tens of μm (Fig. 2A, B). After loading with ibuprofen, no discernable differences in the particles or indications of crystalline ibuprofen on the surface of the particles are observable (Fig. 2C).

### 3.3. Paste extrusion performance

Sample compositions with a range of different ratios between PEG 400 and either unloaded MMC or drug-loaded MMC were first screened for their extrudability and printability performance. After thoroughly

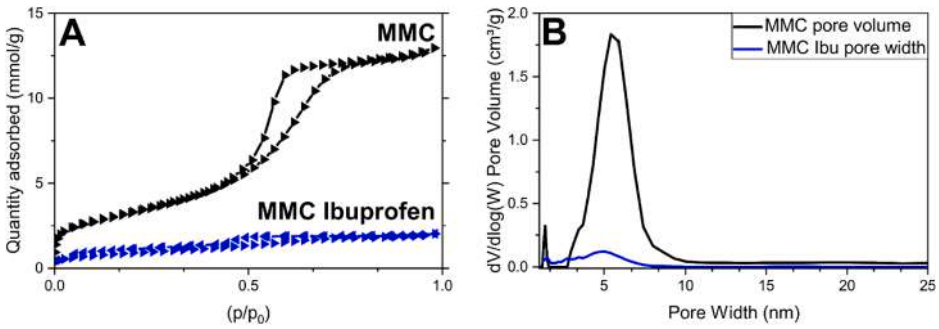


**Fig. 1.** Nitrogen sorption analysis for the unloaded and drug-loaded MMC; panel A: Adsorption and desorption isotherms, panel B: Pore size distribution.

**Table 1**
SSA, pore volume and pore width for unloaded and drug-loaded MMC.

| Sample | SSA $m^2/g$ | Pore volume $cm^3/g$ | Pore width nm |
|---|---|---|---|
| MMC unloaded | 263.7 | 0.43 | 5.43 |
| MMC Ibuprofen | 74.2 | 0.05 | 5.04 |

mixing the components in a mortar, the materials were transferred to syringes and tested for ease of extrusion through a 16-gauge nozzle.

A lower ratio of unloaded MMC/PEG 400 (40/60) resulted in a paste that was extrudable, but unable to be layered or maintain its shape post-extrusion. However, higher ratios of unloaded MMC/PEG 400 (≥50/50) resulted in a grainy substance that had poor flowability and could not be considered a paste. On the other hand, mixtures of drug-loaded MMC and PEG 400 were both extrudable and printable. For example, a 50/50 ratio exhibited an improved performance compared to the same ratio with unloaded MMC. Increasing the drug-loaded MMC component of the mixture resulted in more viscous pastes with improved printability, as they could keep their shape after being extruded from the nozzle. The 60/40 composition of drug-loaded MMC/PEG 400 performed the best while the slightly higher 65/35 ratio formed a firm paste that was too viscous to be able to extrude.

For comparison with the drug-loaded MMC/PEG 400 mixtures, attempts to extrude ibuprofen-loaded mesoporous silica particles (MCM-41, synthesized as previously described [23]) were made. It was found that drug-loaded MCM-41/PEG 400 ratios above 25/75 were not extrudable, and that at a ratio of 25/75 the extruded paste was unable to be layered or maintain its shape post-printing.

### 3.4. Rheological evaluation

Rheology measurements were conducted to evaluate the impact of increasing mesoporous material concentration on viscosity. Fig. 3 illustrates the results of these compositions. As anticipated based on the paste extrusion performance described in Section 3.2, the viscosity increased with higher concentrations of MMC. Furthermore, the materials displayed shear-thinning behavior where the viscosity decreases with increasing shear rate, which is characteristic of the polymer component in the system. Compositions containing more unloaded MMC than the 40/60 ratio or more loaded MMC than the 65/35 ratio displayed non-liquid, grainy behavior, rendering them unmeasurable and consequently they are not included in the viscosity analysis.

The increased viscosity of mixtures with unloaded MMC compared to similar proportions with drug-loaded MMC is likely due to the adsorption of PEG 400 within the pores of MMC, as the hydrodynamic radius of PEG 400 is smaller than the pore size of MMC [32,33]. PEG 400 acts as a lubricant in the system and thus when PEG 400 is absorbed into the pores of MMC, the lubrication effect is diminished and the viscosity of the mixture increases. The pores of unloaded MMC are empty, allowing for a greater amount of PEG 400 to be absorbed compared to the drug-loaded MMC where only a percentage of the pores remain empty as the rest of the pore volume is taken up by the drug. This effect allows for

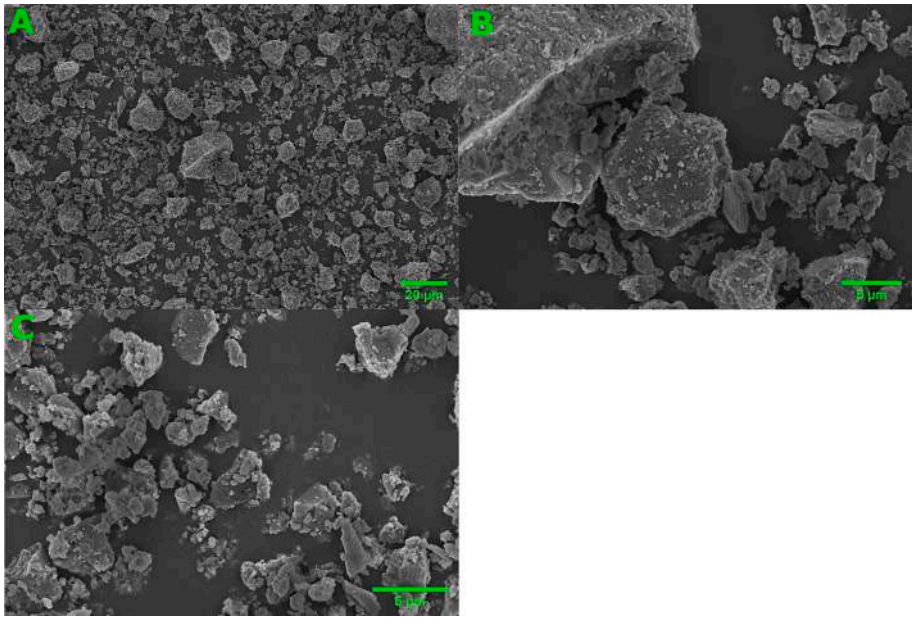


**Fig. 2.** SEM images of MMC. Panels A and B: unloaded MMC, Panel C: MMC loaded with ibuprofen.

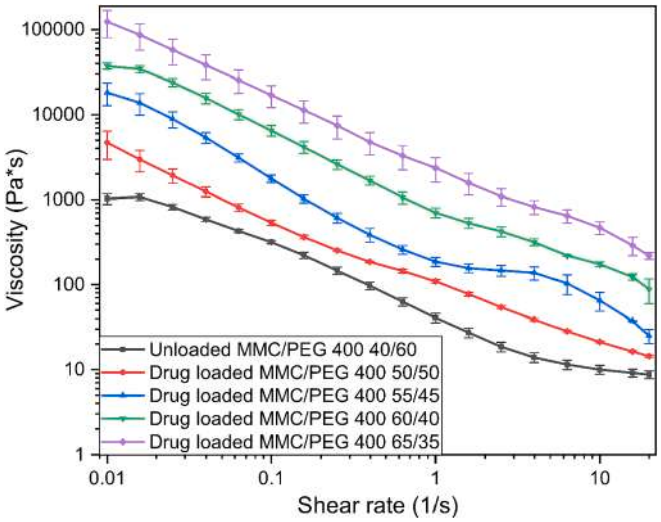


**Fig. 3.** Viscosity measurement with different material compositions. Data expressed as mean ± S.D. (n = 3).

higher ratios of MMC/PEG 400 with drug-loaded MMC while maintaining an extrudable paste. For example, when unloaded MMC was mixed with PEG 400 at a 50/50 ratio the resulting composition was grainy and could not form an extrudable paste while similar issues are only encountered when mixtures of drug-loaded MMC with PEG 400 exceed ratios greater than 60/40. Based on the rheology measurements and the results of the paste extrusion performance outlined in Section 3.2, the paste with a ratio of 60/40 was selected as the optimal composition for printing and subsequent characterization.

To evaluate the stability of the optimal composition over time, viscosity measurements were performed on the 1st, 2nd, and 5th day after mixing. It was observed that the drug-loaded MMC/PEG 400 60/40 sample exhibited an increase in viscosity after 1 day of storage, where the viscosity increased to levels at and above viscosity of the 65/35 ratio sample shown in Fig. 3. Fig. 4 illustrates this increase in viscosity as a function of storage time. The increase in viscosity with storage time suggests that PEG 400 is slowly diffusing into the unoccupied pore volume of the drug-loaded MMC.

### 3.5. Paste printing, weight distribution and morphological assessment

All fabricated formulations used a drug-loaded MMC/PEG 400 mixture ratio of 60/40 and exhibited shape and dimensions in accordance with the respective 3D models (Fig. 5). The printing process for the two different dosage forms was straightforward, however, the samples were too soft to be handled due to the nature of the paste. Commonly, in SSE-produced formulations an extra step of curing, usually drying, is required [25,34–36]. Table 2 presents the average mass of five samples of each printed formulation directly after printing, and after the curing which lasted for 24 h. There was a small but statistically significant increase in mass ($p < 0.01$ for both dosage forms, paired 2-tailed *t*-test), likely attributable to the absorption of moisture from the surrounding air. This also indicates that the curing process does not involve the evaporation of moisture or other volatile substances. Therefore, instead of drying, the curing process involves the adsorption of PEG 400 in the remaining empty pore volume of MMC, as also suggested by the rheological studies. After this curing process, the samples became more rigid and could be handled without deformation. It can also be noted that the printed samples did not change shape or size during the curing process, and points to an advantage of this simple formulation for SSE printing compared to aqueous formulations such as hydrogels, which typically require a drying process post-printing, resulting in a significant loss of weight and change in shape or size of the formulation.

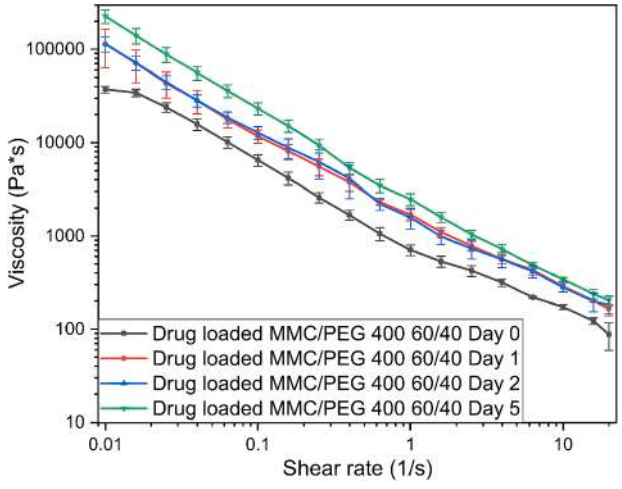


**Fig. 4.** Viscosity of 60/40 drug-loaded MMC/PEG 400 mixture after different storage times as a function of share rate. Data expressed as mean ± S.D. (n = 3).

### 3.6. DSC

The phase transitions of ibuprofen, PEG 400, unloaded and drug-loaded MMC along with the paste were investigated via DSC, and their respective thermograms are presented in Fig. 6. The paste was analyzed both the day of preparation and post-curing, and since no changes were present in the thermogram, only the latter is presented here.

In the thermogram of unloaded MMC a broad endothermic slope is present in the range of 60 to 130 °C due to the evaporation of adsorbed moisture, while ibuprofen's thermogram exhibits a sharp endothermic peak at 78 °C, which corresponds to the drug's melting point [37]. In contrast, post-loading, the MMC Ibuprofen sample presents no thermal events in the range scanned, indicating the successful amorphization of ibuprofen within the pores of MMC, as no melting peaks are observable. PEG 400's melting point is noted at 7 °C, corresponding well with previously reported results [38].The thermogram of the paste formed also exhibits a melting point at 7 °C, corresponding to the PEG 400 component, but no other thermal events are noticeable, indicating the ability of the system to retain the drug in its amorphous form. Lastly, the paste formulation after 12 months of storage at room temperature was also analyzed. The thermogram of this sample is nearly identical to the paste formulation as prepared. A melting point at 7 °C is noted, corresponding to PEG 400 within the paste, and a broad endotherm is noticeable between the range of 70 and 150 °C, due to the evaporation of moisture that has been adsorbed by the paste over the long storage period. There is no melting point ascribed to ibuprofen present, indicating no recrystallization and that the drug remains in the amorphous form within the pores of MMC, even after a long storage period at room temperature.

### 3.7. TGA

TGA was performed to investigate the thermal decomposition of the raw materials and developed paste over the range of temperatures from 25 to 700 °C. The thermograms of ibuprofen, unloaded and drug-loaded MMC, PEG 400 and the paste are depicted in Fig. 7. Ibuprofen exhibits a one-step degradation step with an onset at around 160 °C. A small mass loss of around 4 % is observed until 200 °C for PEG 400, which is attributed to the water content present in the material, while degradation of the polymer begins at around 220 °C. In the case of MMC, an initial mass loss due to moisture being evaporated from the material's pores is observed, followed by a decarbonation process leaving behind MgO [19]. In unloaded MMC the moisture evaporation accounts for 14

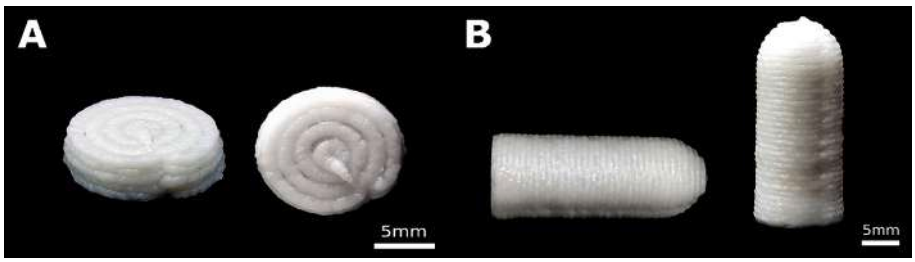


**Fig. 5.** Photos of the printed samples taken with a digital camera. Panel A: Tablet, Panel B: Suppository.

**Table 2**
Mass of the printed samples.

| Sample | Mass after printing (n = 5) | Mass after curing (n = 5) |
|---|---|---|
| Tablet | 516 ± 8 mg | 522 ± 8 mg |
| Suppository | 2.20 ± 0.09 g | 2.23 ± 0.09 g |

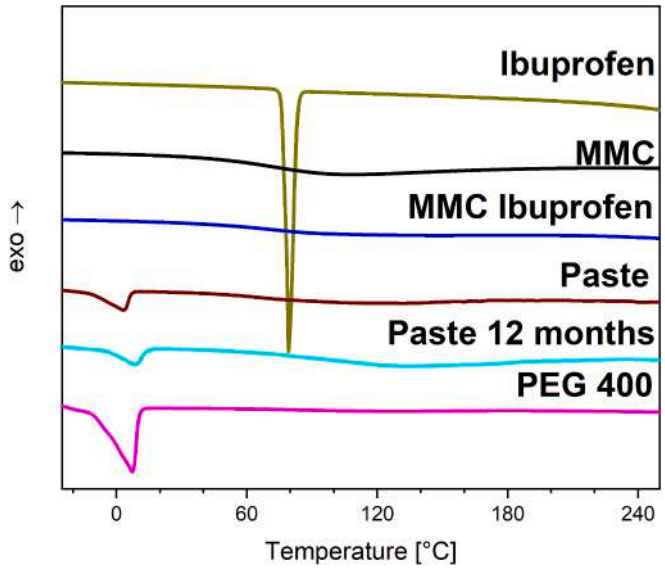


**Fig. 6.** DSC thermograms of the paste and individual components.

% of mass and the decarbonation begins at around 330 °C, resulting in MgO, which accounts for approximately 50 % of the material's initial mass. A similar process is observed for the drug-loaded MMC that also contains a degradation process for the loaded ibuprofen. Its trace reveals a mass loss due to moisture of ~4.5 %, and the decarbonation process has become broader as it incorporates the degradation of ibuprofen, beginning at around 290 °C and ending at ~540 °C, and leaving 40.5 % MgO. This degradation onset is 130 °C higher than the onset of the crystalline ibuprofen powder, indicating a substantial thermal protection effect through incorporation of ibuprofen in the pores of MMC. This effect has been described previously and the approach of protecting thermolabile drugs via mesoporous materials can be a useful alternative for processes performed at elevated temperatures, such as the hot melt extrusion [22,23].

At the end of the heating cycle at 700C both the unloaded and drug-loaded MMC consist only of MgO and can therefore be compared to calculate the drug loading degree of ibuprofen in MMC. As MMC decomposes into $CO_2$ and MgO, the ratio of MgO to the initial MMC weight is constant. An indirect drug loading of MMC can therefore be calculated according to the following equation:

$$MMC_{L(230)} = MgO_L \frac{MMC_{(230)}}{MgO}$$

where $MMC_{L(230)}$ is the theoretical mass percentage of the drug-loaded MMC without drug at 230 °C after the evaporation of moisture, $MgO_L$ is the mass percentage of MgO left from the drug-loaded MMC after its decomposition at 700 °C, $MMC_{(230)}$ represents the mass percentage of the unloaded MMC at 230 °C after the evaporation of moisture, and MgO is the mass percentage of MgO left from the unloaded MMC after its decomposition at 700 °C. By applying this equation on the data collected, the mass percentage of the drug-loaded MMC without drug is calculated to be 40.5 * 86.3/50 % = 69.9 %. The difference between this value and the actual sample mass at 230 °C determined via the TGA trace provides the drug loading degree of ibuprofen in MMC. Specifically, in this case, the drug loading is (95.4–69.9) % = 25.5 %, which matches well to the value of 28.1 % obtained from gas sorption measurements.

Returning to Fig. 7, it can be observed that the TGA trace of the paste is similar to the one of the drug-loaded MMC. A small mass loss of ~4.5 % due to moisture leaving the sample is noted. The decomposition of PEG 400 and ibuprofen with the decarbonation process of MMC appear to overlap in a wide step beginning at around 280 °C and reaching a plateau at 510 °C. Based on the indirect calculations for the drug loading of ibuprofen in MMC via the TGA measurements and knowing that 60 % of the paste consists of loaded MMC, a final loading degree of ibuprofen in the paste, and therefore the printed formulation, is calculated to be 15.3 %. To our knowledge this is the highest loading degree achieved in the final formulation for hydrogels or pastes containing mesoporous materials printed via SSE. Other studies have achieved comparable drug loadings in mesoporous particles (e.g., 6.7 % triamcinolone acetonide loaded in SBA-15 [25] and 23 % clobetasol propionate loaded in MCM-41[26]), but the final loading degree of the drug in the SSE formulations is orders of magnitude less than the loading degree achieved in the present study (e.g., 0.04 % [25] and 0.009 % [26]).

### 3.8. Drug content and in vitro dissolution

This study was focused on the development of a simple paste of a poorly soluble drug loaded in a mesoporous material. The paste that was formed was subsequently printed in two different types of dosage forms, namely, a tablet and a suppository.

Prior to the *in vitro* dissolution study, the drug content of the developed formulations was determined by dissolving them in ethanol (Table 3). The drug loading degree of ibuprofen in MMC was calculated to be 28.6 %, in excellent agreement with the target value of 28.5 % (based on the targeted loading of 90 % of the available pore volume of 0.43 $cm^3/g$, see Table 1). The drug loading values for the tablet and suppository were calculated at 16.6 % and 16.1 %, respectively. Both these values are strikingly close to the theoretical value of 17.1 % (i.e., 60 % of 28.5 %) and highlight the benefit of having a simple formulation platform.

Each formulation's *in vitro* drug release was investigated in a respective biorelevant medium. For both the tablet and the suppository, the dissolution of equivalent doses of crystalline ibuprofen was also studied. The amount of the crystalline drug used was determined via the theoretical loading degree of ibuprofen in the paste, i.e., 15.3 % and the

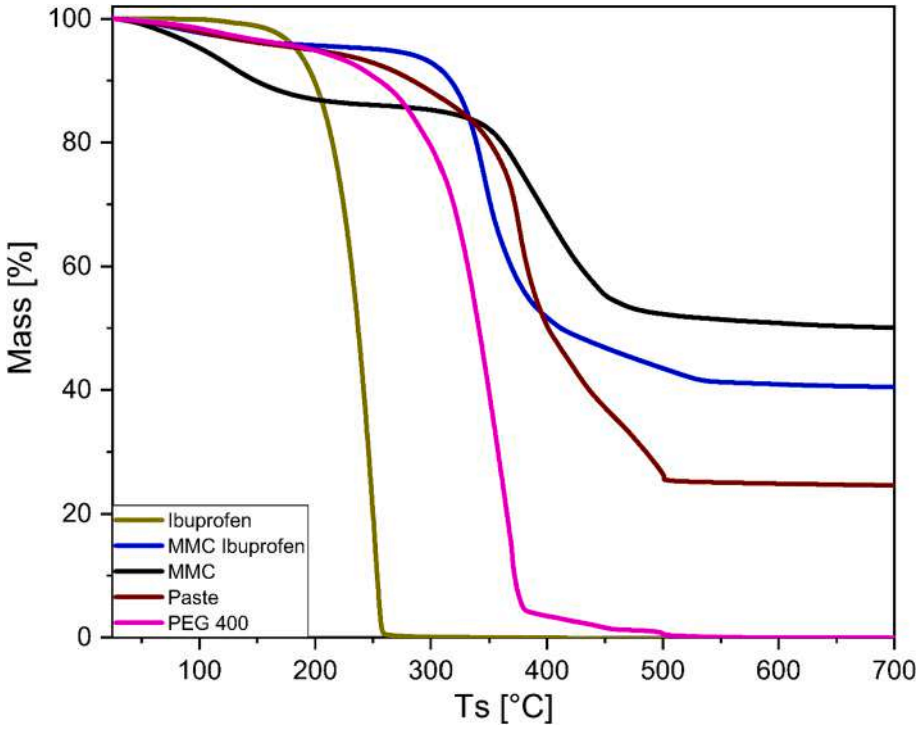


**Fig. 7.** TGA thermograms of the paste and individual components.

**Table 3**
Drug content of the developed formulations.

| Sample | Drug loading w/w (n = 3) |
|---|---|
| MMC Ibuprofen | 28.6 ± 0.9 % |
| Tablet | 16.6 ± 0.7 % |
| Suppository | 16.1 ± 0.7 % |

weight distribution of each formulation (see Table 2). For the tablet 79 mg was used, whereas for the suppository 341 mg was used.

Examining the drug release curves of ibuprofen in SGF (Fig. 8), a significant improvement can be noted between the crystalline form and the printed tablet formulation. A 3- to 10-fold increase was observed in the first hour of release for the concentrations of dissolved ibuprofen achieved. By the end of the two hours of release, the concentration reached by the printed tablet is more than double of that of the crystalline drug. In terms of percentage of drug released, a similar trend is seen. Approximately 26 % of ibuprofen is released from the tablet within the first 10 min of the study compared to ~1 % of the crystalline form. By 60 min, 38 % is reached by the tablet compared to 7 % of the pure ibuprofen. By the end of two hours the percentages of drug released are 40 % and 14 % for the tablet and the crystalline form, respectively. The improvement in concentrations reached, as well as the rate that this was achieved, highlights the significant benefits of amorphizing the drug within the pores of MMC and administering the dosage in this form compared to the crystalline form.

The drug release curves in phosphate buffer at pH 7.4 simulating rectal administration are depicted in Fig. 9. The dissolution of crystalline ibuprofen in this buffer is significantly different than in SGF, and the maximum concentration of ibuprofen is reached after only 20 min. In terms of percentage of drug released, 90 % of crystalline ibuprofen is dissolved within the first 10 min and a plateau of 100 % is achieved after 20 min. The obvious difference in the release behavior of ibuprofen in the two media, SGF and PB, is a consequence of the solubility of the drug

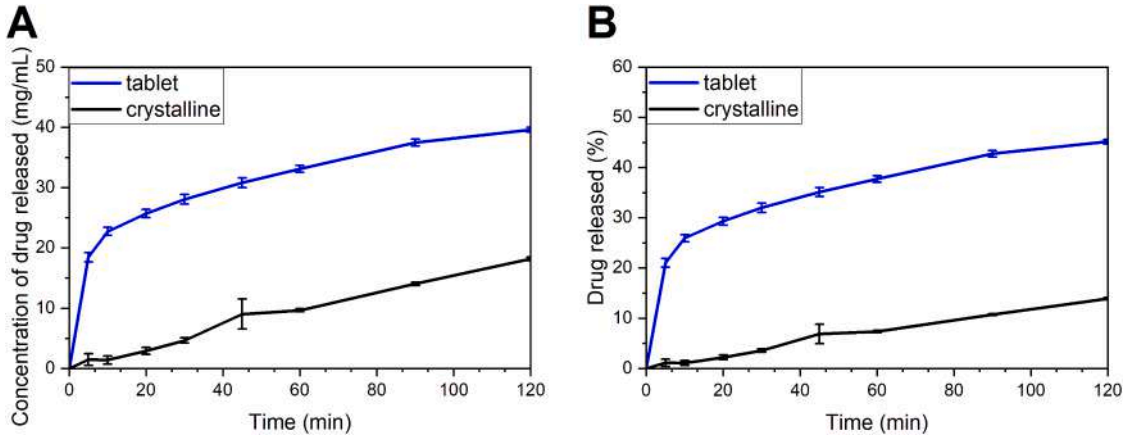


**Fig. 8.** Drug release curves of tablet formulation and equivalent dose of crystalline ibuprofen. Panel A: concentration of drug released over time; Panel B: % drug released over time. Data expressed as mean ± S.D. (n = 3).

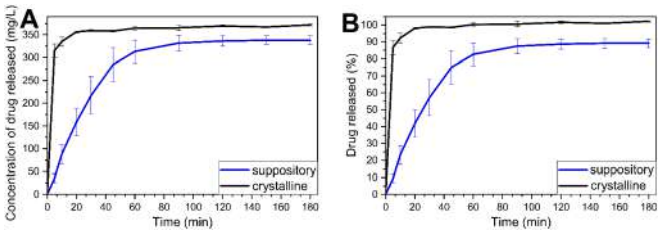


**Fig. 9.** Drug release curves of suppository formulation and equivalent dose of crystalline ibuprofen. Panel A: concentration of drug released over time; Panel B: % drug released over time. Data expressed as mean ± S.D. (n = 3).

at different pH. Ibuprofen is chemically a weak acid and, hence, in lower pH such as 1.2 for SGF its solubility and rate of dissolution is significantly lower than in a phosphate buffer at pH 7.4, *c.f.* Figs. 8 and 9. The dissolution of the 3D-printed suppository is observably slower compared to the crystalline blank experiment. The slower dissolution rate of the suppository can be primarily attributed to surface area. The powder particles of crystalline ibuprofen have a higher surface area and dissolve quicker compared to the suppository which first must disintegrate to expose the ibuprofen to the dissolution media. Furthermore, the crystalline blank experiment contains the equivalent amount of PEG 400 in the release media, which is known to enhance the dissolution of poorly soluble drugs [39,40]. Nevertheless, the dissolution of ibuprofen from the suppository formulation is relatively quick and the release plateau is reached after 60 – 90 min, which is comparable to previous studies of hydrophilic rectal formulations containing ibuprofen [29]. It is therefore shown that the proposed platform of a paste for 3D-printing containing drug-loaded MMC mixed with PEG 400 is a viable alternative for rectal formulations as well, showing a satisfactory release of the drug in an acceptable time frame.

## 4. Conclusions

This study highlights the potential of an innovative hybrid 3D printing system, showcasing its versatility in engineering distinct drug formulations for various administration routes. By harnessing the unique properties of mesoporous magnesium carbonate (MMC), a poorly water-soluble drug was effectively incorporated into its porous structure, transforming it into an amorphous state. This transformation significantly improves the drug's release, paving the way for enhanced bioavailability. Simple blending with PEG 400 produces a flowable and easily manageable paste with a wide range of applications. Moreover, the loading technique and system characteristics enable the highest drug loading compared to similar systems reported. An analysis of dissolution behavior in biorelevant media corresponding to intended administration routes reaffirms the improved dissolution kinetics of the amorphous drug-loaded MMC formulations. These findings underscore the potential of this novel hybrid 3D printing system for developing drug dosage forms, particularly for poorly water-soluble drugs.

## Funding

This work is conducted within the Additive Manufacturing for the Life Sciences Competence Center (AM4Life). The authors gratefully acknowledge financial support from Sweden's Innovation Agency VINNOVA (Grant no: 2019–00029) and the Swedish Science Council (Grant no: 2019–03729).

## CRediT authorship contribution statement

**Christos S. Katsiotis:** Writing – review & editing, Writing – original draft, Visualization, Investigation, Conceptualization. **Evgenii Tikhomirov:** Writing – review & editing, Writing – original draft, Visualization, Investigation. **Christos Leliopoulos:** Writing – review & editing, Writing – original draft, Visualization, Investigation. **Maria Strømme:** Writing – review & editing, Supervision, Funding acquisition, Conceptualization. **Ken Welch:** Writing – review & editing, Supervision, Conceptualization.

## Declaration of Competing Interest

The authors declare that they have no known competing financial interests or personal relationships that could have appeared to influence the work reported in this paper.

## Data availability

Data will be made available on request.

## References

[1] J.M. Ting, W.W.I. Porter, J.M. Mecca, F.S. Bates, T.M. Reineke, Advances in polymer design for enhancing oral drug solubility and delivery, Bioconjug. Chem. 29 (2018) 939–952.
[2] G.L. Amidon, H. Lennernäs, V.P. Shah, J.R. Crison, A theoretical basis for a Biopharmaceutic drug classification: the Correlation of in vitro drug product dissolution and in vivo bioavailability, Pharm. Res. 12 (1995) 413–420.
[3] K.T. Savjani, A.K. Gajjar, J.K. Savjani, Drug solubility: importance and enhancement techniques, ISRN Pharmaceutics. 2012 (2012) 1–10.
[4] J. Brouwers, M.E. Brewster, P. Augustijns, Supersaturating drug delivery systems: the answer to solubility-limited Oral bioavailability? J. Pharm. Sci. 98 (2009) 2549–2572.
[5] P. Zhang, Z. Gómez, T. de la Torre, K. Welch, C. Bergström, M. Strømme, Supersaturation of poorly soluble drugs induced by mesoporous magnesium carbonate, Eur. J. Pharm. Sci. 93 (2016) 468–474.
[6] P. Zhang, Z. Gómez, T. de la Torre, J. Forsgren, C.A.S. Bergström, M. Strømme, Diffusion-controlled drug release from the mesoporous magnesium Carbonate upsalite ®, J. Pharm. Sci. 105 (2016) 657–663.
[7] J. Yang, C. Alvebratt, P. Zhang, Z. Gómez, T. de la Torre, M. Strømme, C.A. S. Bergström, et al., Enhanced release of poorly water-soluble drugs from synergy between mesoporous magnesium carbonate and polymers, Int. J. Pharm. 525 (2017) 183–190.
[8] C.A. McCarthy, R.J. Ahern, R. Dontireddy, K.B. Ryan, A.M. Crean, Mesoporous silica formulation strategies for drug dissolution enhancement: a review, Expert Opin. Drug Deliv. 13 (2016) 93–108.
[9] K.E. Bremmell, C.A. Prestidge, Enhancing oral bioavailability of poorly soluble drugs with mesoporous silica based systems: opportunities and challenges, Drug Dev. Ind. Pharm. 45 (2019) 349–358.
[10] J. Riikonen, W. Xu, V.-P. Lehto, Mesoporous systems for poorly soluble drugs – recent trends, Int. J. Pharm. 536 (2018) 178–186.
[11] M. Vallet-Regí, F. Balas, D. Arcos, Mesoporous materials for drug delivery, Angewandte Chemie International Edition. 46 (2007) 7548–7558.
[12] K. Lan, D. Zhao, Functional ordered mesoporous materials: present and future, Nano Lett. 22 (2022) 3177–3179.
[13] F. Tang, L. Li, D. Chen, Mesoporous silica Nanoparticles: synthesis, biocompatibility and drug delivery, Adv. Mater. 24 (2012) 1504–1534.
[14] B. Muñoz, A. Rámila, J. Pérez-Pariente, I. Díaz, M. Vallet-Regí, MCM-41 organic modification as drug delivery rate regulator, Chem. Mater. 15 (2003) 500–503.
[15] M. Manzano, V. Aina, C.O. Areán, F. Balas, V. Cauda, M. Colilla, et al., Studies on MCM-41 mesoporous silica for drug delivery: effect of particle morphology and amine functionalization, Chem. Eng. J. 137 (2008) 30–37.
[16] J Forsgren, S Frykstrand, K Grandfield, A Mihranyan, M Strømme, A Template-Free, Ultra-Adsorbing, High Surface Area Carbonate Nanostructure, PLoS ONE 8 (2013) e68486.
[17] S. Frykstrand, J. Forsgren, A. Mihranyan, M. Strømme, On the pore forming mechanism of upsalite, a micro- and mesoporous magnesium carbonate, Microporous Mesoporous Mater. 190 (2014) 99–104.
[18] O. Cheung, P. Zhang, S. Frykstrand, H. Zheng, T. Yang, M. Sommariva, et al., Nanostructure and pore size control of template-free synthesised mesoporous magnesium carbonate, RSC Adv. 6 (2016) 74241–74249.
[19] P. Zhang, J. Forsgren, M. Strømme, Stabilisation of amorphous ibuprofen in upsalite, a mesoporous magnesium carbonate, as an approach to increasing the aqueous solubility of poorly soluble drugs, Int. J. Pharm. 472 (2014) 185–191.
[20] E. Mathew, G. Pitzanti, E. Larrañeta, D.A. Lamprou, 3D printing of Pharmaceuticals and drug delivery Devices, Pharmaceutics. 12 (2020) 266.
[21] C.I. Gioumouxouzis, C. Karavasili, D.G. Fatouros, Recent advances in pharmaceutical dosage forms and devices using additive manufacturing technologies, Drug Discov. Today 24 (2019) 636–643.
[22] C.S. Katsiotis, M. Åhlén, M. Strømme, K. Welch, 3D-printed mesoporous Carrier system for delivery of poorly soluble drugs, Pharmaceutics. 13 (2021) 1096.
[23] C.S. Katsiotis, M. Strømme, K. Welch, Processability of mesoporous materials in fused deposition modeling for drug delivery of a model thermolabile drug, International Journal of Pharmaceutics: x. 5 (2023) 100149.

[24] H. Wickström, E. Hilgert, J.O. Nyman, D. Desai, D. Şen Karaman, T. De Beer, et al., Inkjet printing of drug-loaded mesoporous silica Nanoparticles—A platform for drug development, Molecules 22 (2017) 2020.
[25] L.M. Schmidt, J. dos Santos, T.V. de Oliveira, N.L. Funk, C.L. Petzhold, E. V. Benvenutti, et al., Drug-loaded mesoporous silica on carboxymethyl cellulose hydrogel: development of innovative 3D printed hydrophilic films, Int. J. Pharm. 620 (2022) 121750.
[26] R.S. de Oliveira, N.L. Funk, J. dos Santos, T.V. de Oliveira, E.G. de Oliveira, C. L. Petzhold, et al., Bioadhesive 3D-printed skin drug delivery Polymeric films: from the drug loading in mesoporous silica to the Manufacturing process, Pharmaceutics. 15 (2023) 20.
[27] P. Panraksa, S. Qi, S. Udomsom, P. Tipduangta, P. Rachtanapun, K. Jantanasakulwong, et al., Characterization of hydrophilic Polymers as a syringe extrusion 3D printing material for orodispersible film, Polymers 13 (2021) 3454.
[28] C.S. Katsiotis, E. Tikhomirov, M. Strømme, J. Lindh, K. Welch, Combinatorial 3D printed dosage forms for a two-step and controlled drug release, Eur. J. Pharm. Sci. 187 (2023) 106486.
[29] K. Gjellan, C. Graffner, Comparative dissolution studies of rectal formulations using the basket, the paddle and the flow-through methods: II. ibuprofen in suppositories of both hydrophilic and lipophilic types, Int. J. Pharm. 112 (1994) 233–240.
[30] S. Brunauer, L.S. Deming, W.E. Deming, E. Teller, On a theory of the van der waals adsorption of gases, J. Am. Chem. Soc. 62 (1940) 1723–1732.
[31] Ibuprofen | C13H18O2 | ChemSpider [Internet]. [cited 2022 Jan 17]. Available from: http://www.chemspider.com/Chemical-Structure.3544.html.
[32] M.P.J. Dohmen, A.M. Pereira, J.M.K. Timmer, N.E. Benes, J.T.F. Keurentjes, Hydrodynamic radii of polyethylene glycols in different solvents determined from viscosity measurements, J. Chem. Eng. Data 53 (2008) 63–65.
[33] X. Dong, A. Al-Jumaily, I.C. Escobar, Investigation of the use of a bio-derived solvent for non-solvent-induced phase Separation (NIPS) fabrication of polysulfone membranes, Membranes 8 (2018) 23.
[34] Y. Yang, X. Wang, X. Lin, L. Xie, R. Ivone, J. Shen, et al., A tunable extruded 3D printing platform using thermo-sensitive pastes, Int. J. Pharm. 583 (2020) 119360.
[35] S.A. Khaled, M.R. Alexander, R.D. Wildman, M.J. Wallace, S. Sharpe, J. Yoo, et al., 3D extrusion printing of high drug loading immediate release paracetamol tablets, Int. J. Pharm. 538 (2018) 223–230.
[36] S.A. Khaled, M.R. Alexander, D.J. Irvine, R.D. Wildman, M.J. Wallace, S. Sharpe, et al., Extrusion 3D printing of Paracetamol tablets from a single formulation with tunable release profiles through control of tablet geometry, AAPS PharmSciTech 19 (2018) 3403–3413.
[37] G.K. Eleftheriadis, C.S. Katsiotis, D.A. Andreadis, D. Tzetzis, C. Ritzoulis, N. Bouropoulos, et al., Inkjet printing of a thermolabile model drug onto FDM-printed substrates: formulation and evaluation, Drug Development and Industrial Pharmacy. 46 (2020) 1253–1264.
[38] R. Paberit, E. Rilby, J. Göhl, J. Swenson, Z. Refaa, P. Johansson, et al., Cycling stability of poly(ethylene glycol) of six Molecular weights: influence of thermal conditions for energy applications, ACS Appl Energy Mater. 3 (2020) 10578–10589.
[39] M. Newa, K.H. Bhandari, J.O. Kim, J.S. Im, J.A. Kim, B.K. Yoo, et al., Enhancement of solubility, dissolution and bioavailability of ibuprofen in solid dispersion systems, Chem. Pharm. Bull. 56 (2008) 569–574.
[40] M. Newa, K.H. Bhandari, D.X. Li, J.O. Kim, D.S. Yoo, J.-A. Kim, et al., Preparation and evaluation of immediate release ibuprofen solid dispersions using polyethylene glycol 4000, Biol. Pharm. Bull. 31 (2008) 939–945.